Synthesis, characterization and biological activities of S-2- or S-4-methylbenzyl-β-N-(di-2-pyridyl)methylenedithiocarbazate and Cu(II), Ni(II), Zn(II) and Cd(II) complexes

T. B. S. A. Ravoof[a]*, K. A. Crouse[a], E. R. T. Tiekink[b], M. I. M. Tahir[a], E. N. Md. Yusof[a], R. Rosli[c]

[a] *Department of Chemistry, Faculty of Science, Universiti Putra Malaysia, 43400 Serdang, Selangor, Malaysia.*

[b] *Research Centre for Crystalline Materials, School of Science and Technology, Sunway University, Bandar Sunway, 47500 Selangor, Malaysia*

[c] *Department of Biomedical Sciences, Faculty of Medicine and Health Sciences, Universiti Putra Malaysia, 43400 Serdang, Selangor, Malaysia*

**corresponding author: thahira@upm.edu.my*

Metal complexes of general formula, $[M(NNS)_2]$ (M = Cu(II), Ni(II), Zn(II) and Cd(II); NNS' = S-2-methylbenzyl-β-N-(di-2-pyridyl)methylenedithiocarbazate (**1**), NNS''= S-3-methylbenzyl-β-N-(di-2-pyridyl)methylenedithiocarbazate (**2**) and NNS'''= S-4-methylbenzyl-β-N-(di-2-pyridyl)methylenedithiocarbazate (**3**) have been synthesized by reacting the respective metal acetates with the Schiff bases in an ethanol/acetonitrile mixture. They have been characterized by various physico-chemical techniques. Magnetic and spectral evidence indicate the formation of six-coordinate complexes in which the Schiff base coordinates as a uninegatively charged tridentate NNS ligand. The crystal structures of $[Ni(NNS')_2]$ (**5**), $[Ni(NNS''')_2]$ (**13**) and $[Cd(NNS')_2]$ (**7**) were solved *via* single-crystal X-ray crystallographic analysis. All three complexes possess a distorted octahedral geometry where two Schiff bases are coordinated to the central metal ion via the pyridine nitrogen-atom, the azomethine-nitrogen atom and the thiolate-sulphur atom; like donor atoms in the N_4S_2 donor set are mutually *trans*. The complexes have been assayed against selected pathogens and cancer cell lines. The complexes were inactive against all the fungal strains tested, but were mildly active against the bacterial strains tested, especially against *Bacillus subtilis*. Anti-microbial activity generally improved upon complexation with the transition metal ions. The Schiff bases and their transition metal complexes were mostly inactive against the examined

cancer cell lines. The Schiff bases **1-3** were inactive against the MCF-7 (Human Breast cancer cells with positive estrogen receptor) and the MDA-MB-231 (Human Breast cancer cells with negative estrogen receptor) cell lines. Only **9** was active against MCF-7 whereas **10** and **13** were active against the MDA-MB-231 cell line. Cytotoxic activity was observed to be enhanced upon complexation particularly for the Ni(II) complexes.

Keywords: biological activities, S-R-methylbenzyldithiocarbazate, di-2-pyridylketone, Schiff bases

1. Introduction

Dithiocarbazate Schiff bases and their transition metal complexes [1-10] have been of considerable interest to scientists for many years as they show a wide range of therapeutic properties against various diseases, with different anti-bacterial, anti-malarial, anti-viral and anti-tumour properties [1-10]. In recent years, heterocyclic thiosemicarbazones and Schiff bases derived from S-alkyl dithiocarbazates have been considered as useful model compounds for sulphur-containing analogues of purine and pyrimidine bases [11-13]. The π-delocalisation of charge and the configurational flexibility of their molecular chain give rise to a great variety of coordination modes [14-18]. Their chemistry and pharmacological applications have been widely investigated as well [1-6, 15-18].

Coordination compounds, especially those that contain nitrogen-sulphur ligands are synthesized via relatively simple, cost-effective procedures and it has been observed that small changes in their structure, such as change of substituents and their chelation to different metal ions cause great changes in their bioactivities. The coordination of these compounds often lead to enhanced biological activity in several pathogenic fungi [3, 19-21]. Some of these metal complexes have been known to accelerate drug action and the efficacy of a therapeutic agent [1-6, 19-21].

The Schiff bases synthesized in this study are the di-2-pyridylketone Schiff bases of isomeric dithiocarbazates, S-2-methylbenzyldithiocarbazate, S-3-methylbenzyl dithiocarbazate and S-4-methylbenzyldithiocarbazate (Fig. 1).

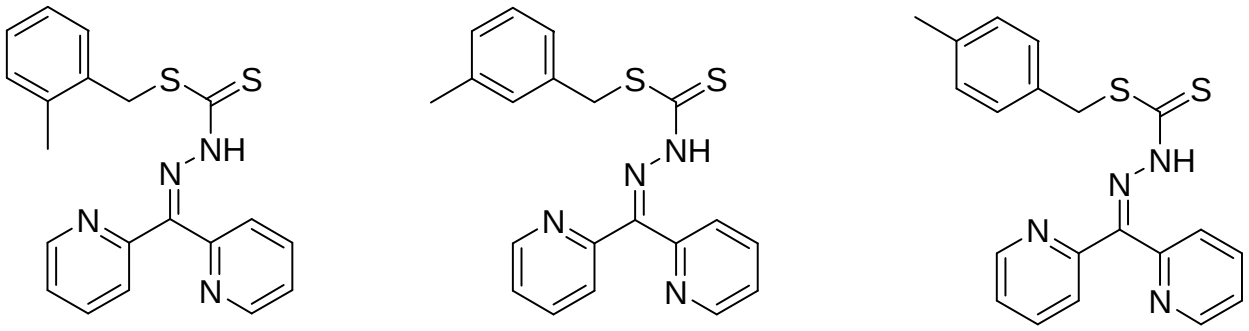

(**1**) (**2**) (**3**)

Fig. 1. Thione forms of the isomeric di-2-pyridylketone Schiff bases

Investigations have shown that di-2-pyridylketone thiosemicarbazone and an analogue, 2-benzoylpyridine thiosemicarbazone, demonstrated marked and selective anti-tumour activity in vitro and also in vivo against many tumours. Di-2-pyridylketone thiosemicarbazone has also been found to possess several structural characteristics important for iron chelating efficacy and potent anti-proliferative activity, and can be further modified as anti-neoplastic agents. Iron has a crucial role in the active site of ribonuclease reductase which is the rate-limiting step of DNA synthesis. This Schiff base and other similar compounds have been found to be well-tolerated by experimental animals in vivo and lead to low toxicity to normal tissues [22-24].

Recently, studies on analogous Schiff bases, di(2-pyridyl)ketone 4,4-dimethyl-3-thiosemicarbazone (Dp44mT) and di(2-pyridyl)ketone 4-cyclohexyl-4-methyl-3-thiosemicarbazone (DpC) showed them to be highly potent and selective anti-tumour and anti-metastatic compounds [25]. Both of these agents had different efficacies and toxicity in vivo. Another study reported that Dp44mT had potential to overcome multi-drug resistance issues in cancer treatment. The drugs had greater activity in drug-resistant tumour cells than their drug-sensitive counterparts [26].

We report herein the synthesis, characterization and biological activities of three novel isomeric dithiocarbazate Schiff bases of di-2-pyridylketone and their Cu(II), Ni(II), Zn(II) and Cd(II) complexes, their bioactivities against selected microbes and breast cancer cells, as well as the X-ray crystallographic analyses of three complexes, i.e. Ni(II) (**5** and **7**) and Cd(II) (**13**).

2. Experimental

2.1. Instrumentation

The analyses for carbon, hydrogen, nitrogen and sulphur were carried out using a LECO CHNS-932 instrument. The IR spectra, as KBr pellets, were recorded on a Perkin-Elmer FT IR 1750X spectrophotometer (4000-400 cm^{-1}). Metal determinations were carried out using a Perkin-Elmer Plasma 1000 Emission Spectrometer. The molar conductance of 10^{-3} M solutions of the metal complexes in DMSO were measured at 29 °C using a Jenway 4310 conductivity meter and a dip-type cell with a platinized electrode. Magnetic susceptibilities at room temperature were measured using a Sherwood Scientific MSB-AUTO magnetic susceptibility balance. The UV-VIS spectra were run on a Shimadzu UV- 2501 PC Recording Spectrophotometer (1000-200 nm).

2.2. Preparation of S-n-methylbenzyldithiocarbazate (n = 2, 3 and 4)

Following a procedure adapted from Ravoof *et al*. [27] and Omar *et al*. [28], potassium hydroxide (11.4 g, 0.2 mol) was dissolved in absolute ethanol (70 ml). To this solution, hydrazine hydrate (10 g, 0.2 mol) was added and the mixture was cooled in an ice-salt bath to 0 °C. Carbon disulphide (15.2 g, 0.2 mol) was added dropwise with constant stirring over a period of 1 h. The two layers that subsequently formed were separated using a separating funnel. The light-brown lower layer was dissolved in 40% ethanol (60 ml) below 5 °C. The mixture was kept in an ice-bath and to it, n-methylbenzyl chloride (n = 2, 3 or 4) (26.5 ml, 0.2 mol) was added dropwise with vigorous stirring of the mixture. The sticky white product which formed was filtered and left to dry overnight in a dessicator over anhydrous silica gel. (Yields: *ca* 85% for each compound, m.p. n = 2: 171.2 °C, n = 3: 132.3 °C and n = 4: 160.0 °C).

2.3. Preparation of S-n-β-N-(di-2-pyridyl)methylenedithiocarbazate [n = 2-methylbenzyl or 3-methylbenzyl or 4-methylbenzyl] (1, 2, and 3)

S-n-dithiocarbazate (0.01 mol, 2.12 g) was dissolved in hot acetonitrile (150 ml). This was added to an equimolar amount of di-2-pyridylketone (0.01 mol, 1.84 g) in ethanol (10 ml). The mixture was heated for 30 mins and then allowed to stand for a few hours or placed in a refrigerator. The bright-yellow crystals that formed were filtered, washed with cold ethanol and recrystallized from acetonitrile. Yields were high, *ca* 85%.

^{1}H-NMR (1): (DMSO-d6, ppm, 14.94 (s, 1H, NH), 7.13 – 7.32 (multiplet, 16H, Ar-H), 4.46 (d, 4H, -SCH_2), 2.35 (s, 3H, -CH_3); ^{13}C-NMR: (DMSO-d6, ppm,), 198.98 (C=S), 164.71 (C=N), 126.15-154.49 (Ar-C), 36.25 (S-CH_2), 18.79 (CH_3). ^{1}H-NMR (2): (DMSO-d6, ppm, 14.94 (s, 1H, NH), 7.22 – 8.85 (multiplet, 13H, Ar-H), 4.48 (s, 2H, -SCH_2), 2.28 (s, 3H, -CH_3); ^{13}C-NMR: (DMSO-d6, ppm,), 199.08 (C=S), 148.70 (C=N), 123.61-148.70 (Ar-C), 38.25 (S-CH_2), 20.94 (CH_3). ^{1}H-NMR (3): (DMSO-d6, ppm, 15.25 (s, 1H, NH), 7.10 – 7.95 (multiplet, 13H, Ar-H), 4.44 (s, 2H, -SCH_2), 2.26 (s, 3H, -CH_3); ^{13}C-NMR: (DMSO-d6, ppm,), 199.33 (C=S), 154.50 (C=N), 123.55-150.47 (Ar-C), 36.75 (S-CH_2), 20.69 (CH_3). Mass data m/z(%) (1/2/3): $[M]^+$ 378(0.40/0.06/0.03), $[C_{12}H_{10}N_4S]^+$ 240(-/24.25/23.57), $[C_{12}H_{12}N_4]^+$ 211(0.40/10.54/12.09), $[C_{11}H_8N_3]^+$ 183(0.03/5.71/3.27), $[C_8H_{10}S]^+$ 138(0.22/41.19/21.97), $[C_6H_5N_2]^+$ 105(100.0/100.0/100.0), $[C_7H_8]^+$ 91(2.65/6.05/5.02), $[C_5H_5N]^+$ 78(4.79/55.52/55.77).

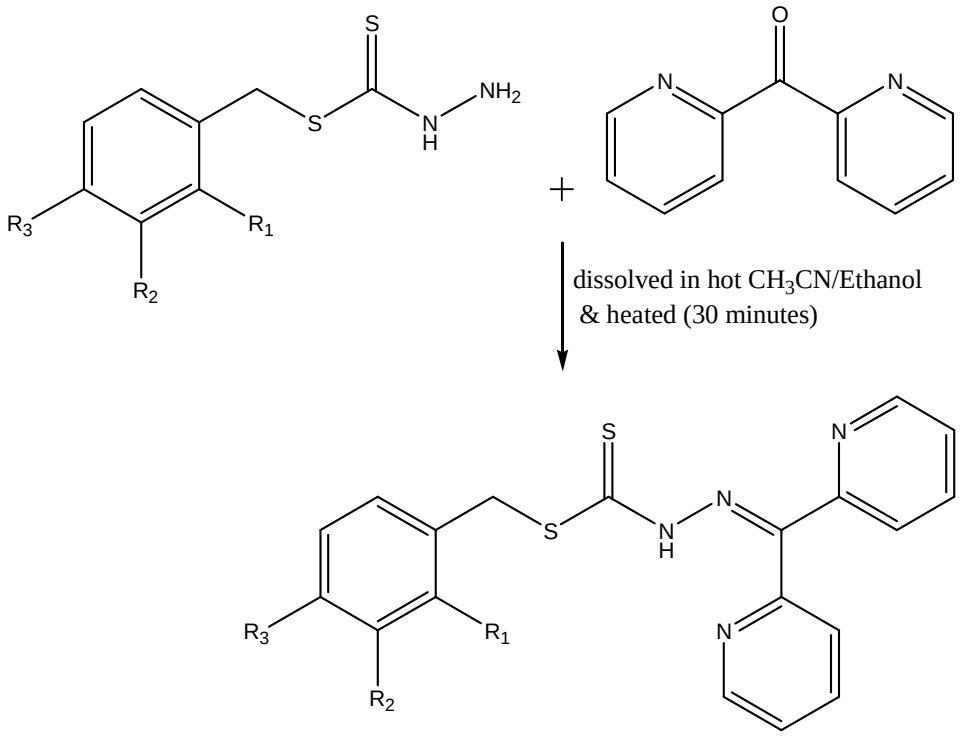

Where;

	R_1	R2	R_3
1 =	CH_3	H	H
2 =	H	CH_3	H
3 =	H	H	CH_3

Scheme 1. General synthesis of the isomeric Schiff bases

2.4. General method of synthesis of the transition-metal complexes (4-15)

The transition metal salts used were the acetate salts of Cu(II), Ni(II), Cd(II) and Zn(II) (0.001 mol) which was dissolved in hot ethanol (10 ml) and mixed with a solution of the Schiff base (0.002 mol, 0.76 g) in acetonitrile (100 ml) The resulting mixture was heated for 30 mins. On standing overnight, the mixture yielded crystalline complexes which were filtered off and dried overnight in a desiccator over anhydrous silica gel. Yields: *ca* 70%. Crystals of **5**, **7** and **13** suitable for X-ray diffraction analysis were obtained from acetonitrile solution over one week. Analytical, physical and spectral data on the complexes are displayed in Tables 2 and 3.

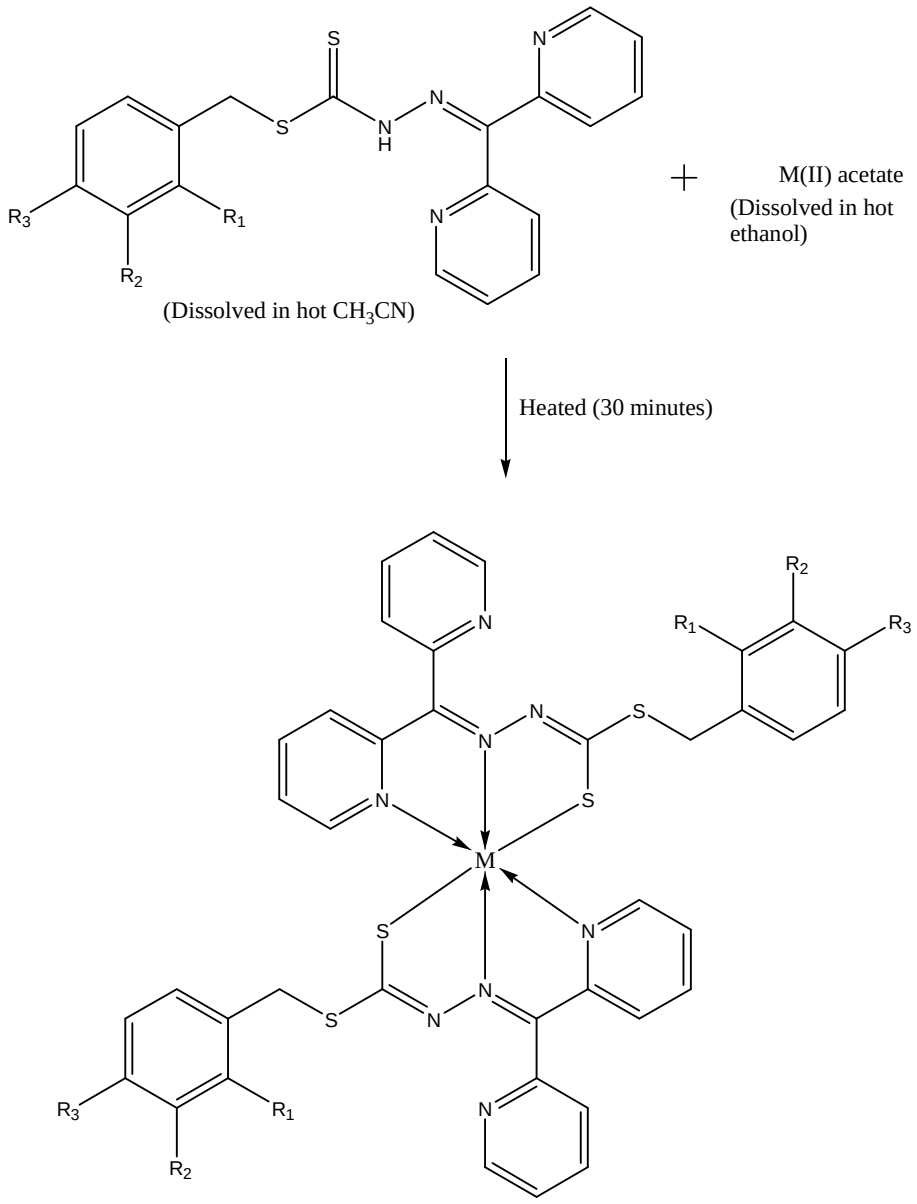

Scheme 2. General synthesis of the metal complexes

2.5. X-ray crystallography analysis

Intensity data for **5**, **7** and **13** were measured at 150 K on a Nonius Kappa CCD diffractometer using MoKα radiation, λ = 0.71073 Å [29]. The structures were solved by direct methods (SHELXS97 [30] through the WinGX Interface [31]) and refined (anisotropic displacement parameters, C-bound H atoms in the riding model approximation and a weighting scheme of the form $w = 1/[\sigma^2(F_o^2) + aP^2 + bP]$ where $P = (F_o^2 + 2F_c^2)/3$) with SHELXL2014/7 on F^2 [32]. The molecular structure diagrams shown in Figs 2-4 were drawn with 70% displacement ellipsoids for **5** and 50% for each of **13** and **7** [31]. Crystallographic data are collated in Table 1. The crystal packing diagrams were generated with DIAMOND [33] with additional crystallographic analysis employing PLATON [34].

Table 1

Summary of the crystallographic data for **5**, **7**, and **13**.

	5	**13**	**7**
Formula	$C_{40}H_{34}N_8NiS_4$	$C_{40}H_{34}N_8NiS_4$	$C_{40}H_{34}CdN_8S_4$
Formula weight	813.70	813.70	867.39
Crystal size (mm)	0.06 x 0.10 x0.46	0.10 x 0.20 x 0.30	0.24 x 0.30 x 0.32
Crystal system	monoclinic	monoclinic	monoclinic
Space group	*C*2/*c*	$P2_1/n$	*C*2/*c*
a/Å	22.7123(6)	15.5569(4)	22.8859(3)
b/Å	13.0429(4)	16.0046(5)	13.0785(2)
c/Å	14.7375(4)	16.7904(4)	15.1730(2)
α/°	90	90	90
β/°	120.8310(10)	112.023(2)	121.3720(10)
γ/°	90	90	90
V/Å^3	3748.79(19)	3875.47(19)	3877.54(10)
Z/*Z*'	4/0.5	4/1	4/0.5
D_c/g cm^{-3}	1.442	1.395	1.486
μ/mm^{-1}	0.783	0.757	0.820
θrange/°	5.2–27.5	5.1–27.9	5.1–27.5
Reflections measured	8048	8246	8027
Independent reflections; R_{int}	4251, 0.034	6420, 0.038	4417, 0.014
Reflections with $I > 2\sigma(I)$	3236	6240	4002
Number of parameters	241	480	241
R, obs. data; all data	0.036, 0.058	0.040, 0.066	0.026, 0.030

a; *b* in wght scheme	0.052; 0	0.033; 2.727	0.043; 2.072
R_w, obs. data; all data	0.084, 0.093	0.087, 0.097	0.069, 0.072
GoF (F^2)	1.01	1.04	1.04
$\Delta\rho_{max,\ min}$ (e Å^{-3})	0.49, -0.46	0.33, -0.62	0.74, -0.56
CCDC Nos	1492224	1492225	1492226

2.6. Bioactivity

2.6.1. Target microorganisms

Seven pathogenic microbials were used to test the biological potential of the complexes. They were Methicillin resistant *staphylococcus* (MRSA), *Bacillus subtilis* wild type (*B. Sub*), *Pseudomonas aeruginosa* (*P. aer*), *Salmonella Choleraesuis* (*S. cho*) *Candida albicans* (C. A.), *Aspergillus ochraceous* (*A. Och*) and *Saccaromyces cerevisiae* (*S.Cere*). The source of the microbes and culture maintenance were as previously described [35].

2.6.2. Qualitative anti-microbial assay

Anti-microbial activity of each sample was qualitatively determined by a modified disc diffusion method [36] as previously detailed [37]. A lawn of microorganisms was prepared by pipetting and evenly spreading inoculum (10^{-4} cm^3, adjusted turbidometrically to $10^5 – 10^6$ cfu cm^3 (cfu: colony forming units) on to agar set in Petri dishes, using Nutrient agar (NA) for the bacteria and potato dextrose agar (PDA) for fungi. Whatman No. 1 filter paper discs of 6 mm diameter were impregnated with a stock solution of the trial compound (100 mg cm^{-3}) and dried under sterile conditions. The dried discs were then placed on the previously inoculated agar surface. The plates were inverted and incubated for 24h at 30 °C for bacteria and 37 °C for fungi. Anti-microbial activity was indicated by the presence of clear inhibition zones around the discs. Commercially available streptomycin (Sigma, USA) was used for the anti-bacterial control while nystatin (Sigma, USA) was used as the anti-fungal control.

2.6.3. Quantitative anti-microbial assay.

Compounds that showed positive (diameter >15 mm) anti-microbial inhibition with the disc diffusion assay were subjected to the broth dilution method for the quantitative measurement of microbiostatic (inhibitory) activity as described by Hufford and Clark [38]. The lowest concentration that completely inhibited visible microbial growth was recorded as the

minimum inhibitory concentration (MIC, µg/ml). Streptomycin and nystatin were used as controls for bacteria and fungi, respectively.

2.6.4. Cytotoxic assay

The MCF-7 (Human breast cancer cells with positive estrogen receptor) and MDA-MB-231 (Human breast cancer cells with negative estrogen receptor) cell lines were obtained from the National Cancer Institute, U.S.A. The cells were cultured in RPMI-1640 / DMEM (High glucose) (Sigma) medium supplemented with 10% fetal calf serum. Cytotoxicity was determined using the microtitration of 3-(4,5-dimethylthiazol-2-yl)-2,5-diphenyl tetrazolium bromide (MTT) assay (Sigma, USA) as reported by Mosmann [35]. Controls that contained only cells were included for each sample. Cytotoxicity was expressed as IC_{50}, i.*e*. the concentration that reduced the absorbance of treated cells by 50% with reference to the control (untreated cells). Tamoxifen was used as the standard cytotoxin.

3. Results and discussion

3.1. Synthesis

The physicochemical properties of the Schiff bases (**1**-**3**) and their metal complexes (**4**-**15**) together with their analytical data are shown in Table 2. The three isomeric Schiff bases only differ from each other in the position of a methyl group (CH_3) attached to the benzene ring. The analytical data (Table 2) indicated good agreement with the proposed formulations for the compounds. The complexes were soluble in most organic solvents and appeared to be stable in air. The complexes adopted a six-coordinate geometry containing two tridentate NNS Schiff bases.

Table 2

Analytical data and physical properties of the HNNS Schiff bases (**1**-**3**) and their metal complexes (**4**-**15**)

Compound	Colour	M.p (°C)	Λ [a]	µ [b]	Analytical data (%) [c]				
					C	H	N	S	M
HNNS' (**1**)	Light-yellow	87	-	-	62.97 (63.46)	4.68 (4.79)	14.57 (14.80)	17.96 (16.94)	-
HNNS'' (**2**)	Yellow	147	-	-	63.35 (63.46)	4.71 (4.79)	14.24 (14.80)	16.87 (16.94)	-
HNNS''' (**3**)	Light-yellow	127	-	-	62.85 (63.46)	4.74 (4.79)	14.15 (14.80)	17.24 (16.94)	-
[Cu(NNS')$_2$] (**4**)	Dark-green	166	9.63	1.98	58.67 (58.69)	4.22 (4.19)	13.65 (13.69)	15.42 (15.67)	7.65 (7.76)

[Ni(NNS')$_2$] (**5**)	Brown	244	7.20	3.02	59.60 (59.0)	4.17 (4.21)	13.54 (13.77)	15.47 (15.76)	7.04 (7.21)
[Zn(NNS')$_2$] (**6**)	Yellow	247	8.73	diam.	58.15 (58.56)	4.25 (4.18)	13.28 (13.66)	15.26 (15.63)	7.65 (7.97)
[Cd(NNS')$_2$] (**7**)	Yellow	199	4.54	diam.	55.02 (55.39)	3.89 (3.95)	13.25 (12.92)	15.02 (14.79)	12.78 (12.96)
[Cu(NNS'')$_2$] (**8**)	Dark-green	168	12.12	1.74	58.34 (58.69)	4.49 (4.19)	13.04 (13.69)	15.21 (15.67)	7.69 (7.76)
[Ni(NNS'')$_2$] (**9**)	Dark-brown	280	11.39	2.87	58.93 (59.04)	4.12 (4.21)	13.24 (13.77)	15.12 (15.76)	7.14 (7.21)
[Zn(NNS'')$_2$] (**10**)	Yellow	234	9.04	diam.	57.88 (58.56)	4.09 (4.18)	13.24 (13.66)	15.64 (15.63)	7.91 (7.97)
[Cd(NNS'')$_2$] (**11**)	Orange	238	8.94	diam.	55.15 (55.39)	3.86 (3.95)	13.06 (12.92)	15.14 (14.79)	12.65 (12.96)
[Cu(NNS''')$_2$] (**12**)	Green	134	12.18	1.65	58.19 (58.69)	4.02 (4.19)	13.77 (13.69)	16.04 (15.67)	8.02 (7.76)
[Ni(NNS''')$_2$] (**13**)	Golden-green	221	8.84	2.82	59.25 (59.04)	4.15 (4.21)	13.25 (13.77)	14.98 (15.76)	6.96 (7.21)
[Zn(NNS''')$_2$] (**14**)	Yellow	227	6.49	diam.	57.96 (58.56)	4.25 (4.18)	13.96 (13.66)	15.02 (15.63)	7.06 (7.97)
[Cd(NNS''')$_2$] (**15**)	Yellow	177	10.98	diam.	54.96 (55.39)	4.02 (3.95)	13.41 (12.92)	14.22 (14.79)	12.68 (12.96)

[a] Molar conductance (Ω^{-1} cm^2 mol^{-1}) of ca 10^{-3} M solutions in DMSO;

[b] Magnetic moments at 298 K in B.M.; [c] Calculated values are given in parentheses

3.2. Magnetic and conductivity data

The magnetic moments of the copper(II) complexes at room temperature were in the range of 1.65-1.98 B.M, as expected for a $3d^9$ metal ion in a magnetically dilute environment [1-6]; Table 2. The nickel(II) complexes exhibited magnetic moments ranging from 2.82 to 3.02 B.M. According to previous studies [3, 39], octahedral nickel(II) complexes with two unpaired electrons will have magnetic moments between 2.9 and 3.4 B.M which indicates a small but definite orbital contribution to the magnetic moment. The magnetic moments of the zinc(II) and cadmium(II) complexes were found to be diamagnetic, which indicated distorted octahedral structures [40]. All the complexes were non-electrolytes in DMSO, evidence that the two ligands moieties did not dissociate in solution [41]. The conductivity data supported the coordination of the two Schiff bases to the metal ion and the absence of free ions in solution [42].

3.3. Infrared and electronic spectra

Important and characteristic IR absorptions are given in Table 3. The IR spectra of the ligands exhibited *v*(C=N), *v*(N-N) and *v*(CSS) bands at *ca* 1584-1632, 964-1082 and 944-966 cm^{-1}, respectively. These bands shifted in the spectra of the metal complexes indicating the coordination of the ligands to the metal ions via the pyridine-nitrogen, azomethine-nitrogen and thiolate-sulphur atoms. The coordination of the azomethine-nitrogen to metal ions was

indicated by the shifting of the *v*(C=N) band to lower frequencies and the shift of the *v*(N-N) band to higher frequencies [42]. The lowering of the *v*(C=N) band was due to the M-N formation, which lowered the C=N bond order [1-6, 40-43]. However, in the spectrum of the [Cu(NNS')$_2$] complex, the *v*(C=N) band shifted from lower to higher frequency as has been observed in other reports [1-6, 40-44]. The *v*(N-N) bands of the Schiff bases shifted from lower to higher wavenumbers upon complexation due to the reduction in the repulsion between the lone pairs of electrons on the nitrogen atoms as a result of the coordination through the azomethine-nitrogen atom [1-6, 43]. The shift of *v*(CSS) bands to higher frequencies in the complexes indicated the coordination *via* one of the sulphur atoms. The absence of the *v*(NH) band in the spectra of the metal complexes suggested that the ligand lost one proton on complexation, thus acting as a uninegatively charged ligand [40].

The electronic spectral data for all compounds are tabulated in Table 3. The electronic spectra of the complexes in DMSO exhibited intra-ligand bands which was attributed to the $n\rightarrow\pi^*$ transition in the 360-275 nm range and S→M(II) charge transfer bands in the 440-400 nm range. The presence of the S→M(II) LMCT band confirmed the coordination of the Schiff base to the metal ion *via* its thiolate-sulphur atom [1-6, 45]. Nickel(II) and copper(II) complexes exhibited low intensity bands in the 704-600 nm range, which was attributed to weak *d-d* transition bands, consistent with complexes that have six-coordinate geometry [46]. Meanwhile, the zinc(II) and cadmium(II) complexes did not exhibit any *d-d* transitions as they have d^{10} configurations [47] and normally only exhibit intra-ligand and charge-transfer transitions [40].

Table 3

Selected IR bands and electronic spectral data of the HNNS Schiff bases (**1**-**3**) and their metal complexes (**4**-**15**)

Compound	IR bands (cm^{-1})				Electronic spectra (In DMSO) λ max (log ε)
	v(C=N)	*v*(N-N)	*v*(CSS)	*v*(NH)	
1	1584 s	964 s	958 m	3052 w	280 (3.20)
2	1608 m	1058 s	944 m	3036 w	320 (3.19), 360 (3.48)
3	1632 m	1082 s	966 w	3030 w	275 (3.08), 300 (2.88), 400 (3.08)
4	1594 s	1074 s	985 m	-	275 (3.00), 330 (2.85), 430 (2.90), 675 (1.40)
5	1584 m	1088 s	996 s	-	292 (2.38), 350 (2.19), 437 (1.99), 704 (0.30)

6	1582 s	1090 s	982 m	-	300 (3.10), 330 (2.95), 410 (2.88)
7	1562 s	1080 s	985 m	-	300 (2.90), 330 (2.85), 400 (2.85)
8	1590 m	1092 s	994 m	-	360 (3.11), 440 (2.90)
9	1588 m	1092 s	980 m	-	320 (3.20), 360 (3.26), 440 (3.18)
10	1588 m	1086 s	976 m	-	330 (2.95), 360 (3.11), 400 (3.13)
11	1596 m	1090 s	976 m	-	320 (3.00), 360 (3.18), 400 (3.20)
12	1590 m	1090 s	979 s	-	280 (3.00), 330 (2.84), 420 (2.54), 685 (1.40)
13	1596 m	1088 s	981 s	-	280 (3.10), 340 (3.08), 425 (2.95), 600 (1.30)
14	1582 m	1090 s	988 s	-	275 (2.88), 350 (3.00), 400 (3.00)
15	1560 m	1092 s	994 s	-	300 (3.20), 390 (1.93)

3.4. Structural commentary

The molecular structure of **5** is shown in Fig. 2 and selected geometric parameters are listed in Table 4. The nickel(II) atom is located on a crystallographic twofold axis of symmetry and is chelated by two deprotonated **1** ligands resulting in a neutral complex formulated as **5**.

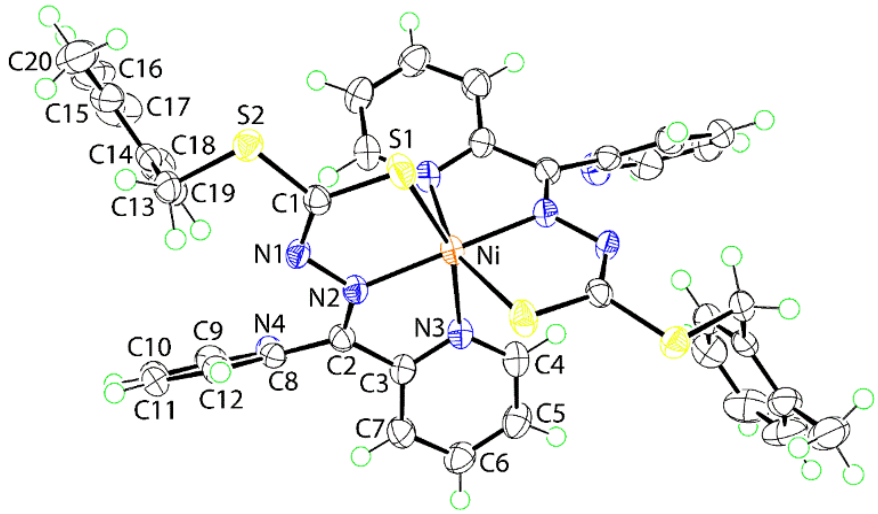

Fig. 2 Molecular structure and atom labelling scheme for **5**. The Ni atom lies on a crystallographic twofold axis. Unlabelled atoms are related by the symmetry operation 1-*x*, *y*, ½-*z*.

The anion derived from **1** is tridentate, coordinating the nickel(II) centre via the thiolate-sulphur, the azomethine-nitrogen and one of the pyridyl-nitrogen atoms; the second pyridyl-nitrogen atom is non-coordinating. The Ni–N(azomethine) bond length is shorter than the Ni–N(pyridyl) bond, Table 4. The tridentate ligand spans meridional positions in a distorted octahedron and defines two five-membered chelate rings hinged at the Ni–N2 bond. The Ni,S1,C1,N1,N2 chelate ring is non-planar (r.m.s. deviation = 0.144 Å), having an envelope conformation with the nickel(II) atom being the flap atom. Similarly, the Ni,N2,C2,C3,N3 ring is twisted about the C2–C3 bond (r.m.s. deviation = 0.095 Å); the dihedral angle between the best planes through the rings is 4.85(7)°. The arrangement of the ligand donors is such that like-atoms occupy mutually trans positions, Table 4.

The molecular structure of the isomeric analogue **13**, is shown in Fig. 3 and geometric data given in Table 4. Complex **13** lacks the molecular symmetry of **5** but, the overall structure is in essential agreement with that just described. There some experimentally distinct differences in chemically equivalent bond lengths, most notably in the Ni–S1, S3 separations of 2.3952(6) and 2.4257(6) Å, respectively, which are shorter and longer, respectively, than the equivalent bonds in **5**, i.e. 2.4159(5) Å. There is a close concordance in the key bond angles in **5** and **13** with the exceptions being in the N2–M–N6 and N3–M–N7 angles which are wider and narrower, each by about 5°, in **5** cf. **13**, Table 4.

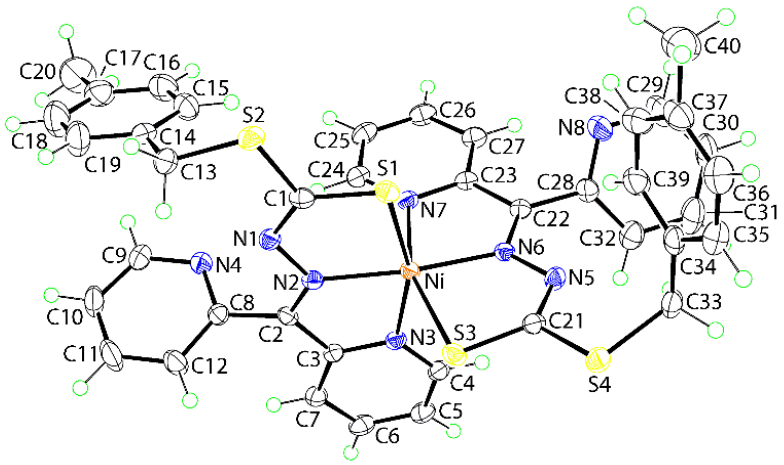

Fig. 3 Molecular structure and atom labelling scheme for **13**.

Crystals were also obtained for **7** which proved to be isostructural with **5**, thereby also having crystallographic twofold symmetry, the molecular structure and data of which are represented in Fig. 4 and Table 4, respectively.

Table 4

Summary of the key geometric (Å, °) data for **5**, **7** and **13**.

	5; M = Ni	**13**; M = Ni	**7**; M = Cd
M–S1	2.4159(5)	2.3952(6)	2.5635(4)
M–N2	2.0241(15)	2.0000(18)	2.3328(12)
M–N3	2.1310(16)	2.0986(19)	2.4334(13)
M–S3	2.4159(5)[a]	2.4257(6)	2.5635(4)[b]
M–N6	2.0241(15)[a]	1.9961(18)	2.3328(12)[b]
M–N7	2.1310(16)[a]	2.1236(18)	2.4334(13)[b]
N1–N2	1.394(2)	1.376(3)	1.3871(19)
N5–N6	1.394(2)[a]	376(3)	1.3871(19)[b]
C1–S1	1.7160(19)	1.708(2)	1.7304(15)
C1–S2	1.7572(19)	1.757(2)	1.7561(16)
C21–S3	1.7160(19)	1.703(2)	1.7304(15)
C21–S4	1.7572(19)[a]	1.762(2)	1.7561(16)[b]
C1–N1	1.307(2)	1.316(3)	1.304(2)
C21–N5	1.307(2)[a]	1.314(3)	1.304(2)[b]
C2–N2	1.298(2)	1.296(3)	1.286(2)
C22–N6	1.298(2)[a]	1.302(3)	1.286(2)[b]
S1–M–N2	81.57(4)	82.07(5)	76.19(3)
S1–M–N3	159.11(4)	160.51(5)	144.89(3)
S3–M–N6	81.57(4)[a]	82.05(5)	76.19(3)[b]
S3–M–N7	159.11(4)[a]	159.89(5)	144.89(3)[b]
N2–M–N3	77.81(6)	78.54(7)	68.72(4)
N6–M–N7	77.81(6)[a]	78.12(7)	68.72(4)[b]
S1–M–S3	94.87(3)[a]	92.82(2)	107.39(2)[b]
N2–M–N6	166.18(9)[a]	171.31(7)	151.12(7)[b]
N3–M–N7	95.81(8)[a]	89.73(7)	91.02(7)[b]

[a] Symmetry-related atoms are generated by the symmetry operation: 1-*x*, *y*, ½-*z*.

[b] Symmetry-related atoms are generated by the symmetry operation: 1-*x*, *y*, 1½-*z*.

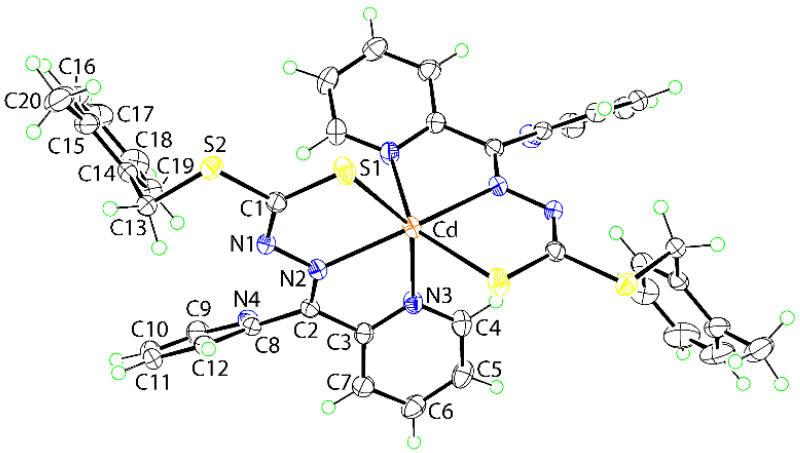

Fig. 4 Molecular structure and atom labelling scheme for **7**. The Cd atom lies on a crystallographic twofold axis. Unlabelled atoms are related by the symmetry operation 1-*x*, *y*, 1½-*z*.

The major difference between the molecular structure of **7** and the nickel(II) analogues, **5** and **13**, rests with the distortions from octahedral geometry, in particular as manifested in the S1–M–N3 and N2–M–N6 bond angles which are narrower in **7** by about 15° cf. **5**.

The molecular packing of **5** is dominated by C–H…S and C–H…π interactions. Supramolecular zigzag chains along the c-axis are sustained by pendent-pyridyl-C–H…S(thioether) and methylene-C–H…S(thiolate) interactions as shown in Fig. 5; geometric parameters associated with these interactions are collated in Table 5. The chains are linked into a three-dimensional architecture by pyridyl-C–H…π(tolyl) and tolyl-C–H…π(pendent pyridyl) interactions, Fig. SI 42.

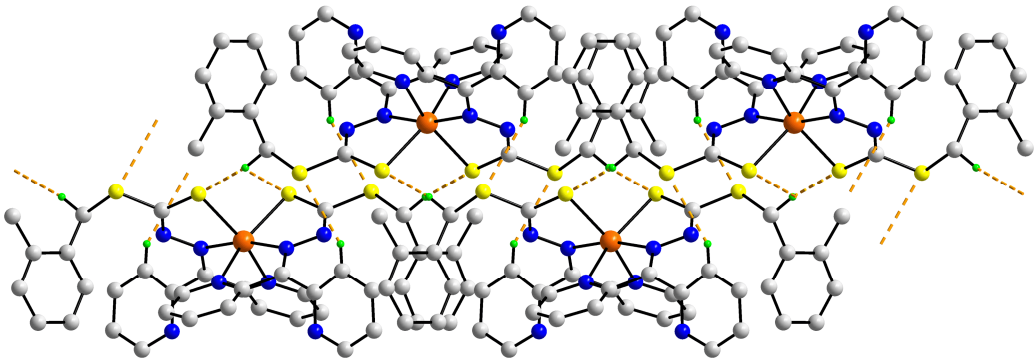

Fig. 5. A supramolecular zigzag chain in the crystal of **5**, aligned along the *c*-axis sustained by C–H…S interactions (non-participating hydrogen atoms have been removed).

A wider range of intermolecular interactions contribute to the molecular packing of **13**. The presence of pyridyl-C–H…S(thioether) and tolyl-C–H…N(pyridyl) interactions combine to generate jagged supramolecular layers parallel to the ab-plane, Fig. 6. These are connected via methylene-, methyl-C–H…π(pyridyl) and pyridyl-C–H…π(tolyl) interactions as well as π…π interactions between pyridyl rings (Table 5) to consolidate the three-dimensional packing, Fig. SI 43.

Table 5

Summary of the key geometric (Å, °) parameters characterising the identified intermolecular contacts in the crystals of **5**, **7** and **13**.

5:

A	H	B	H···B	A···B	A–H···B	Symmetry operation for B
C12	H12	S2	2.85	3.729(2)	154	1-x, 1-y, 1-z
C13	H13b	S1	2.57	3.448(2)	147	x, 1-y, ½+z
C11	H11	Cg(C14-C19)[a]	2.93	3.622(3)	131	1-x, y, 1½-z
C20	H20a	Cg(N4, C8-C12)	2.91	3.774(3)	147	½+x, 1½-y, ½+z.

13:

C11	H11	S4	2.87	3.785(3)	161	-x, 1-y, 1-z
C36	H36	N4	2.60	3.421(3)	145	-1+x, 1½-y, -½+z
C13	H13b	Cg(N3, C3-C7)	2.76	3.688(3)	156	x, 1½-y, -½+z
C30	H30	Cg(C34-C39)	2.93	3.738(4)	143	x, 1½-y, ½+z
C40	H40a	Cg(N4,C8-C12)	2.86	3.826(3)	168	-1+x, 1½-y, -½+z
Cg(N3,C3-C7)	–	Cg(N7,C23-C27)	–	3.6562(13)	8.79(11)[b]	-x, -½+y, 1½-z.

7:

C12	H12	S1	2.86	3.7348(19)	154	1-x, 1-y, 1-z
C13	H13b	S1	2.76	3.6908(18)	157	x, 1-y, -½+z
C11	H11	Cg(C14-C19)	2.93	3.634(2)	132	1-x, y, ½-z
C20	H20a	Cg(N4, C8-C12)	2.99	3.858(3)	149	-½+x, 1½-y, -½+z

a: Cg is the centre of gravity of the specified ring; b: is the angle of inclination between rings

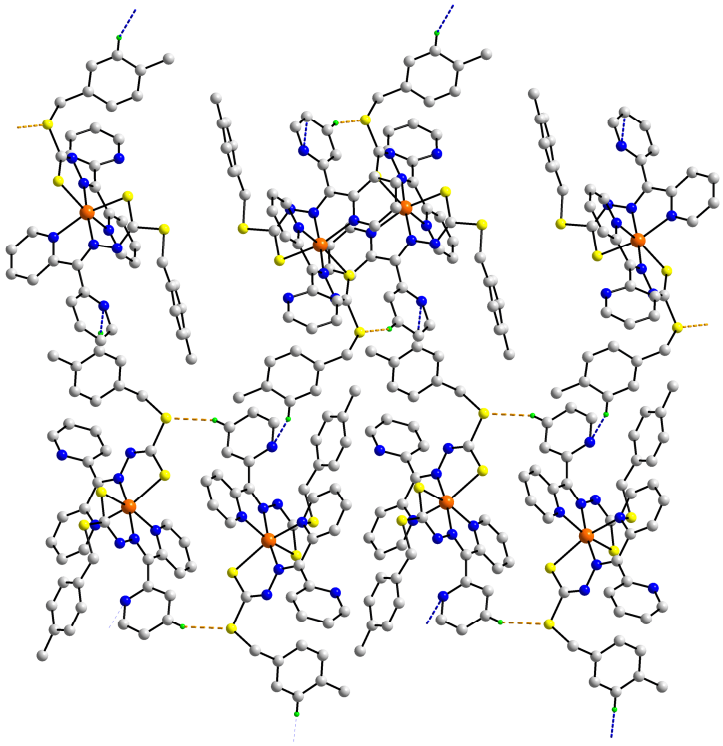

Fig. 6. A supramolecular layer parallel to the ab-plane in the crystal of **13**, sustained by C–H…S and C–H…N interactions (non-participating hydrogen atoms have been removed).

Finally, despite being isostructural with **5**, the molecular packing in **7** presents distinct features. In **7**, supramolecular chains with a zigzag topology are found and these mediated by C–H…S interactions with pyridyl- and methylene-hydrogen atom donors as in **5** but in **7**, these involve the thiolate-S1 atoms only, Fig. SI 44, Table 5. The chains are connected into a three-dimensional architecture by pyridyl-C–H…π(tolyl) and methyl-C–H…π(pyridyl) interactions, Fig. 7, which closely resembles the molecular packing in **5** (see Fig. SI 42).

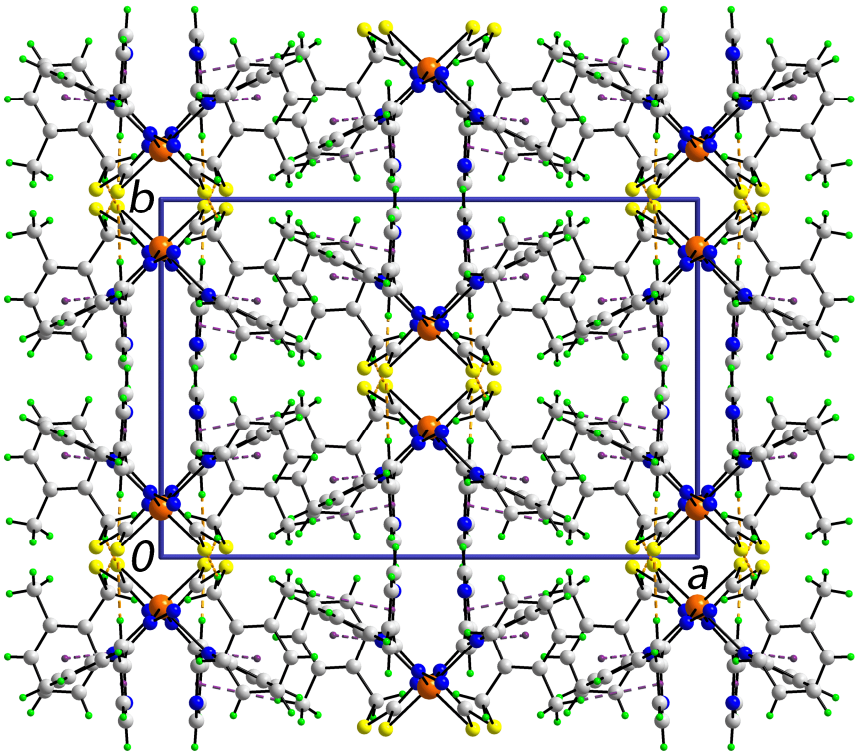

Fig. 7. A view in projection down the *c*-axis of the unit cell contents for **7**. The C–H…S and C–H…π interactions are shown as orange and purple dashed lines, respectively.

3.5. Biological activities

3.5.1. Anti-microbial activities

All of the complexes have been assayed against several selected bacteria and fungi to evaluate their anti-bacterial and anti-fungal potential. The data tabulated in Table 6 indicate that most of the complexes were inactive against all chosen pathogens (inhibitory zones <15 mm). All the three Schiff bases were inactive against the microbes assayed. The compounds in this study were also inactive towards all the fungal strains tested [*Candida albicans* (C.A.), *Aspergillus ochraceous* (*A.Och*) and *Saccaromyces cerevisiae* (*S.Cere*)]

Complex **8** was slightly active against the bacterial strains, while **4** and **12** were only active against *Bacillus subtilis* (*B. Sub*). Complex **15** was also strongly active against the bacterial strains tested while **5** was active against only MRSA. Many of the complexes were found to be active against *Bacillus subtilis* (*B. Sub*). Only **5**, **8**, **13** and **15** were selected for quantitative anti-bacterial analysis. The data obtained indicated that the complexes that were anti-bacterial had MIC values (minimum inhibitory concentration, μg/mL) that were much higher than

streptomycin indicating that they were not as effective, as a higher concentration was needed in order to be lethal against the bacterial strains tested. The MIC values are tabulated in Table 7. However, all the inhibition zones obtained were lower than those observed in the anti-bacterial activities of other related S-methyldithiocarbazate (SMDTC) and S-benzyldithiocarbazate (SBDTC) complexes [48].

Table 6

Qualitative anti-bacterial assay data[a] (inhibition diameter in mm)

Compound	MRSA	*P. aer*	*S. cho*	*B. sub*
3	-	-	-	12
4	-	-	-	12
5	22	-	-	-
6	-	-	-	12
7	-	-	-	12
8	10	6	6	18
10	-	-	-	10
12	-	-	-	10
13	-	-	-	16
14	-	-	-	12
15	-	20	23	23
Streptomycin	20	20	24	23
Nystatin	-	-	-	-

Bacteria: *MRSA* – Methicillin-resistant *Staphylococcus aureus*, *P. aer* – *Pseudomonas aeruginosa*, *S. cho* – *Salmonella cholerasuis*, *B. sub* – *Bacillus subtilis* - wild type

[a] Inhibition diameter > 15 mm is strongly active; - indicates 'not active'

Table 7

Quantitative anti-bacterial assay data[a]

Compound	MIC values (µg/mL)			
	MRSA	*P. aer*	*S. cho*	*B. sub*
5	3125	-	-	-
8	-	-	-	1562

13	-	-	-	781
15	-	391	391	781
Streptomycin	12.2	12.2	17.0	48.8
Nystatin	-	-	-	-

[a] MIC (µg/mL) = minimum inhibitory concentration, *i.e*. the lowest concentration to completely inhibit microbial growth.

3.5.2. Cytotoxic activities

The cytotoxicity data of the Schiff bases and their metal complexes are given in Table 8. All complexes have been examined for their cytotoxicity against two human breast cancer cell lines, MCF-7 and MDA-MB-231 where MCF-7 is a estrogen, progesterone receptor-positive, HER2 negative cell line while MDA-MB-231 is a triple negative (ER, PR and HER2) breast cancer cell line. MCF-7 is a perfect model for hormone therapy while MDA-MB-231 is a perfect model for chemotherapy. Because of their properties, only certain drugs can be effective to treat the particular cancer cells and often, the mechanism of action of these synthesised drugs occur through different pathways in both the cell lines.

Most of the compounds including the Schiff bases were found to be inactive against both cancer cells with IC_{50} values >25 µg/ml. Complex **4** had moderate activity towards MDA-MB-231 and weak activity against MCF-7, with IC_{50} values of 9.5 and 12.0 µg/ml, respectively. It was interesting to note that **9** was strongly active (0.4 µg/ml) against MCF-7 but showed no activity towards MDA-MB-231. Meanwhile, the closely-related **13** was moderately active against MDA-MB-231 but inactive against MCF-7. The latter pattern was also observed for **10**. Thus, only a small change in the backbone of the structure of a complex can change the ability of the complex to act as an anti-cancer agent to different cell lines, in this case, the positioning of the methyl group and the nature of the metal ion [42]. Complexes **7**, **11** and **15** were notably inactive when assayed against both cancer cells. The findings in this work mimic earlier reports of bioactivities of first row transition metal complexes where cytotoxic activity of the complexes is affected by the nature of the constituent metal ion and ligand [49, 50]. The IC_{50} values of the standard, Tamoxifen, were between 5.0 and 5.5 µm/ml.

Table 8

Cytotoxic assay data (IC_{50} values in µg/ml)

Complex	IC_{50} (μg/ml)[a]	
	MCF-7[b]	MDA-MB-231[c]
4	12.0	9.5
6	15.0	>5.0
9	0.4	>5.0
10	>5.0	0.4
13	>5.0	4.0
Tamoxifen	5.0	5.5

[a]IC_{50} is the cytotoxic dose at 50%, i.e. the concentration required to reduce growth of cancer cells by 50%. IC_{50} values < 5.0 μg/ml indicate that the complex is strongly active whereas IC_{50} values of 5.0-10.0, 10.0-25.0 and > 25.0 μg/ml indicate that the complex is moderately active, weakly active and inactive, respectively.

[b]MCF-7 (Human Breast carcinoma with positive estrogen receptor)

[c]MDA-MB-231 (Human Breast carcinoma with negative estrogen receptor)

4. Conclusions

The reaction of isomeric tridentate Schiff bases derived from isomericdithiocarbazates and a heterocyclic ketone with metal acetates in an ethanol/acetonitrile mixture produced beautifully crystalline coloured nickel(II), copper(II), zinc(II) and cadmium(II) complexes in high yields. These complexes had six-coordinate geometries in which the Schiff bases acted as uninegatively charged tridentate ligands, and with like-atoms being mutually *trans*. The X-ray crystal structure determination of **5**, **7** and **13** showed that the complexes had slightly distorted octahedral geometry where the metal ion was coordinated to two tridentate NNS ligands. Most of the complexes in this study had weak potential as anti-microbial agents and showed selective and specific activities as anti-cancer agents when examined against human breast cancer cell lines. As the biological properties of structurally similar dithiocarbazate complexes are of much interest, it would be worthwhile to study the structure-bioactivity relationship of these complexes *in-silico,* to elucidate potential mechanisms of action.

4. Supplementary material

Crystallographic data for the structural analysis have been deposited with the Cambridge Crystallographic Data Centre, CCDC No. 1492224 (**5**), 1492225 (**13**) and 1492226 (**7**). Copies of this information may be obtained free of charge from The Director, CCDC, 12

Union Road, Cambridge, CB2 1EZ, UK (fax: +44-1223-336033; e-mail: deposit@ccdc.cam.ac.uk or www: http://www.ccdc.cam.ac.uk).

Acknowledgements

We thank the Department of Chemistry, the Molecular Genetics Laboratory and Chemical Crystallography Laboratory of Universiti Putra Malaysia (UPM) for providing the laboratory facilities and X-ray crystallographic services. This research was funded by Universiti Putra Malaysia (UPM) and the Malaysian Government under the Intensification of Research in Priority Areas Scheme (IRPA grant No. 09-02-04-0296) and the Malaysian Fundamental Research Grant Scheme (FRGS No. 01–01-16-1833FR).

References

[1] M. L. Low, L. Maigre, M. I. M. Tahir, E. R. T. Tiekink, P. Dorlet, R. Guillot, T. B. S. A. Ravoof, R. Rosli, J. M. Pages, C. Policar, N. Delsuc and K. A. Crouse, Eur. J. Med. Chem. 12 (2016) 1.

[2] N. Nanjundan, R. Narayanasamy, S. Geib, K. Velmurugan, R. Nandhakumar, M. D. Balakumaran and P. T. Kalaichelvan, Polyhedron, 110 (2016) 203.

[3] M. A. A. Islam, M. C. Sheikh, M. A. Mumit, R. Miyatake, M. A. Alam and M. A. O. Mondal, J. Coord. Chem. 69 (2016) 3580.

[4] E. N. Md Yusof, T. B. S. A. Ravoof, E. R. T. Tiekink, A. Veerakumarasivam, K. A. Crouse, M. I. M Tahir and H. Ahmad, Int. J. Mol. Sci. 16 (2015) 11034.

[5] E. N. Md Yusof, T. B. S. A. Ravoof, E. R. T. Tiekink, A. Veerakumarasivam, K. A. Crouse, M. I. M Tahir and H. Ahmad, Inorg. Chim. Acta. 438 (2015) 85.

[6] M. L. Low, G. Paulus, P. Dorlet, R. Guillot, R. Rosli, N. Delsuc, K. A. Crouse, C. Policar, BioMetals. 28 (2015) 553.

[7] M. A. Ali, A. H. Mirza, T. B. S. A. Ravoof and P. V. Bernhardt, Polyhedron 23 (2004) 2031.

[8] F. R. Pavan, P. I. D. S. Maia, S. R. Leite, V. M. Deflon, A. A. Batista, D. N. Sato, S. G. Franzblau, C. Q. F. Leite. Eur. J. Med. Chem. 45 (2010) 1898.

[9] E. Zangrando, M. S. Begum, M. C. Sheikh, R. Miyatake, M. M. Hossain, M. M. Alam, M. A. Hasnat, M. A. Halim, S. Ahmed, M. N. Rahman, A. Ghosh. Arab. J. Chem. 10 (2017) 172.

[10] H. P. Zhou, D. M. Li, P. Wang, L. H. Cheng, Y. H. Gao, Y. M. Zhu, J. Y. Wu, Y. P. Tian, X. T. Tao, M. H. Jiang and H. K. Fun, J. Mol. Struct. 826 (2007) 205.

[11] N. Gandhi, A. Kumar, C. Kumar, N. Mishra, P. Chaudhary, N. K. Kaushik and R. Singh, Main Group Chemistry 15 (2015) 35.

[12] S. Roy, T. N. Mandal, A. K. Barik, S. Pal, S. Gupta, A. Hazra, A., R. J. Butcher, A. D. Hunter, M. Zeller and S. K. Kar, Polyhedron 26 (2007) 2603.

[13] S. Roy, T. N. Mandal, A. K. Barik, S. Gupta, R. J. Butcher, M. Nethaji and S. K. Kar, Polyhedron 27 (2008) 593.

[14] A. H. Mirza, M. A. Ali, P. V. Bernhardt and I. Asri, Polyhedron 81 (2014) 723.

[15] R. K. Dani, M. K. Bharty, S.K. Kushawaha, O. Prakash, V. K. Sharma, R. N. Kharwar, R. K. Singh and N. K. Singh, Polyhedron 81 (2014) 261.

[16] M. X. Li, L. Z. Zhang, C. L. Chen, J. Y. Niu and B.S. Ji, J. Inorg. Biochem. 106 (2012) 117.

[17] S. B. Kalia, V. Sharma, K. Lumba, G. Kaushal and A. Sharma, Indian J. Pharm. Sci. 69 (2007) 438.

[18] B. K. Koo, Bull. Korean Chem. Soc. 32 (2011) 1729.

[19] S. Shrivastava and M. Srivastava, Futuristic Trends in Engineering, Science, Humanities, and Technology FTESHT-16 2 (2016) 1.

[20] S. Rakshit, D. Palit, S. K. Hazari, S. Rabi, T. G. Roy, F. Olbrich and D. Rehder, Polyhedron 117 (2016) 224.

[21] V. Rajurkar, V. Deshmukh and M. Sonawane, Anal. Chem. Lett. 6 (2016) 470.

[22] Z. Debebe, T. Ammosova, D. Breuer, D. B. Lovejoy, D. S. Kalinowski, P. K. Karla, K. Kumar, M. Jerebtsova, P. Ray, F. Kashanchi, V. R. Gordeuk, D. R. Richardson and S. Nekhai, Mol. Pharmacol. 70 (2011) 185.

[23] Y. Yu, Y. S. Rahmanto, C. L. Hawkins, and D. R. Richardson, Mol. Pharmacol. 79 (2011) 921.

[24] D. S. Kalinowski, Y. Yu, P. C. Sharpe, M. Islam, Y. T. Liao, D. B. Lovejoy, N. Kumar, P. V. Bernhardt, D. R. Richardson, J. Med. Chem. 50 (2007) 3716.

[25] V. Sestak, J. Stariat, J. Cermanova, E. Potuckova, J. Chladek, J. Roh, J. Bures, H. Jansova, P. Prusa, M. Sterba, S. Micuda, T. Simunek, D. S. Kalinowski, D. R. Richardson and P. Kovarikova, Oncotarget 6 (2015) 42411.

[26] P. J. Jansson, T. Yamagishi, A. Arvind, N. Seebacher, E. Gutierrez, A. Stacy and D. R. Richardson, J. Biol. Chem. 15 (2015) 9588.

[27] T. B. S. A. Ravoof, K. A. Crouse, M. I. M. Tahir, R. Rosli, D. J. Watkins and F. N. F. How, Transit. Metal Chem. 35 (2010) 871.

[28] S. A. Omar, T. B. S. A. Ravoof, M. I. M. Tahir and K. A. Crouse, Transit. Metal Chem. 39 (2014) 119.

[29] Z. Otwinowski and W. Minor, Method. Enzymol. 276 (1997) 307.

[30] G. M. Sheldrick, ActaCrystallogr., Sect. A. 64 (2008) 112.

[31] L. J. Farrugia, J. Appl. Crystallogr. 45 (2012) 849.

[32] G. M. Sheldrick, Acta Crystalllogr. Sect. C. 71 (2015) 3.

[33] K. Brandenburg, DIAMOND, Crystal Impact GbR, Bonn, Germany, 2006.

[34] A. L. Spek, J. Appl. Crystallogr. 36 (2003) 7.

[35] T. Mosmann, J. Immunol. Methods. 65 (1983) 55.

[36] A. W. Bauer, M. D. K. Kirny, J. C. Sherries and M. Turck, Am. J. Clin. Pathol. 45 (1966) 493.

[37] Z. Yugeng, W. Yebin and Y. Heng, Cryst. Res. Technol. 30 (1995) 831.

[38] C. D. Hufford and A.M. Clark, Studies in Natural Product Chemistry 2 (1988) 421.

[39] P. Nithya, S. Helena, J. Simpson, M. Ilanchelian, A. Muthusankar and S. Govindarajan, J. Photochem. Photobiol. B, Biol. 165 (2016) 220.

[40] M. T. H. Tarafder, A. Kasbollah, K. A. Crouse, A. M. Ali, B. M. Yamin and H. K. Fun, Polyhedron 20 (2001) 2363.

[41] W. J. Geary, Coord. Chem. Rev. 7 (1971) 81.

[42] T. B. S. A. Ravoof, K. A. Crouse, M. I. M. Tahir, A. R. Cowley and M. A. Ali, Polyhedron 26 (2004) 1159.

[43] M. T. H. Tarafder, T. J. Khoo, K. A. Crouse, A. M. Ali, B. M. Yamin and H. K. Fun, Polyhedron 21 (2002) 2691.

[44] M. A. Ali and S. E. Livingstone, Coord. Chem. Rev. 13 (1974) 101.

[45] B. P. Straughan and S. Walker, Spectroscopy, vol 1, Wiley, USA, 1976.

[46] M. J. Bew, B. J. Hathaway and R. J. Fereday, J. Chem. Soc. Dalton Trans. 12 (1972) 1229.

[47] H. T. Sadeq, Journal of Al-Nahrain University 16 (2013) 72.

[48] K. B. Chew, M. T. H. Tarafder, K. A. Crouse, A. M. Ali, B. M. Yamin and H. K. Fun, Polyhedron 23 (2004) 1385.

[49] M. X. Li, L. Z. Zhang, C. L. Chen, J. Y. Niu and B. S. Ji, J. Inorg. Biochem. 106 (2012) 117.

[50] M. Ghosh, M. Layek, M. Fleck, R. Saha and D. Bandyopadhyay, Polyhedron 85 (2015) 312.